ELSEVIER

Journal of Luminescence 92 (2001) 73–78

JOURNAL OF LUMINESCENCE

www.elsevier.com/locate/jlumin

Synthesis and photoluminescence enhancement of Mn^{2+}-doped ZnS nanocrystals

Song Wei Lu[a], Burtrand I. Lee[a,*], Zhong Lin Wang[b], Wusheng Tong[c], Brent K. Wagner[c], Wounjhang Park[c], Christopher J. Summers[c]

[a] *Department of Ceramic and Materials Engineering, Olin Hall, P.O. Box 340907, Clemson University, Clemson, SC 29634-0907, USA*
[b] *School of Materials Science and Engineering, Georgia Institute of Technology, Atlanta, GA 30332-0245, USA*
[c] *Phosphor Technology Center of Excellence, Georgia Institute of Technology, Atlanta, GA 30332-0560, USA*

Received 30 November 1999; received in revised form 4 April 2000; accepted 26 May 2000

Abstract

Mn^{2+}-doped ZnS nanoparticles were synthesized by a chemical precipitation method at room temperature. The particle size was estimated to be 2.8 nm from high-resolution transmission electron microscopy (HRTEM) and calculated as 2.6 ± 0.4 nm from peak broadening of the X-ray diffraction (XRD) pattern. A 30-fold increase in photoluminescence intensity has been observed from Mn^{2+}-doped ZnS nanoparticles after surface passivation by a passivating agent with carboxylic functional groups.

Keywords: Nanocrystal; Mn^{2+}-doped ZnS; Photoluminescence enhancement; Surface passivation

1. Introduction

Doped semiconductor nanocrystals have attracted extensive research interests in the recent years due to their unique optical properties and potential applications [1,2]. Numerous researchers have investigated the structural and luminescent properties of doped phosphor nanoparticles [3–5], especially Mn^{2+}-doped ZnS nanocrystals [1,2,6–9]. However, the discovery of a new class of luminescence materials of doped nanocrystals combining high luminescence efficiency and decay time shortening, as suggested by Bhargava et al. [1,2], has been disputed recently by Bol and Meijerink [10], and Murase et al. [11]. It has been experimentally confirmed that the shortened decay time to several nanoseconds originates from the purple/blue emission of ZnS nanocrystals, which is not related to Mn^{2+} centers in ZnS nanocrystals [10,11]. Indeed, the high photoluminescence (PL) of Mn^{2+}-doped ZnS nanocrystals is still remaining as an interesting research field.

Mn^{2+}-doped ZnS nanoparticles have been synthesized by using chemical precipitation method [1,2,12–16], micro-emulsion method [17], precipitation in a solid polymer matrix [18], and the sol–gel processing followed by reaction with H_2S gas [19]. The doping of Mn^{2+} into ZnS lattice was achieved during the precipitation at room temperature in the solution [1,2], or during the reaction of cations with H_2S gas at an elevated temperature up to 200°C [19]. Methacrylic acid

*Corresponding author. Tel.: +1-864-656-5348; fax: +1-864-656-1453.

E-mail address: burt.lee@ces.clemson.edu (B.I. Lee).

0022-2313/01/$ - see front matter
PII: S0022-2313(00)00238-6

(MA) has been used as a surfactant in order to prevent nanoparticle agglomeration in the solution [1,2,20]. PL enhancement up to ten-fold has been observed for poly methyl methacrylate (PMMA)-coated ZnS nanocrystals doped with Mn^{2+} ions [14,16].

The PL enhancement mechanism for Mn^{2+}-doped ZnS nanoparticles covered with a surface modifying agent has not been systematically discussed in the literature, especially the role of a surface adsorbate on PL enhancement. The objective of this work was to study and discuss the luminescence enhancement effect of Mn^{2+}-doped ZnS nanoparticles by a surface adsorbate. To achieve the luminescence enhancement, 3-methacryloxypropyl trimethoxysilane (MPTS) was used as a surface passivating ligand after chemical precipitation of Mn^{2+}-doped ZnS nanoparticles at room temperature. MPTS was chosen as a surface passivation agent for Mn^{2+}-doped ZnS nanocrystals since it has carboxylic groups in its structure, which has a potential to enhance PL [14,16]. Moreover, the silane group is expected to link individual nanoparticles after surface passivation. The nanostructures of Mn^{2+}-doped ZnS nanocrystals were examined by high-resolution transmission electron microscopy (HRTEM) and X-ray diffraction (XRD) techniques. In this paper, PL enhancement of Mn^{2+}-doped ZnS nanoparticles was observed and is discussed.

2. Experimental

Mn^{2+}-doped ZnS nanocrystals were synthesized by a chemical precipitation method at room temperature using $Zn(CH_3COO)_2 \cdot 2H_2O$, $Mn(CH_3COO)_2 \cdot 4H_2O$, and $Na_2S \cdot 9H_2O$ as starting materials. A 50 ml ethanol solution was prepared by dissolving 2.195 g $Zn(CH_3COO)_2 \cdot 2H_2O$ and 0.049 g $Mn(CH_3COO)_2 \cdot 4H_2O$ with stirring at room temperature. This yielded a Mn^{2+} doping concentration of 2 mol%. Then, a 50 ml aqueous solution of 2.451 g $Na_2S \cdot 9H_2O$ was added to the ethanol solution drop by drop with vigorous stirring. The resultant white precipitate was centrifuged and washed using deionized water. Finally, 1.987 g 3-methacryloxypropyl trimethoxysilane (MPTS) was added to the resultant mixture after centrifuging and washing. In order to compare the effect of a passivating additive on luminescence properties, 0.5 g polyoxyethylene (20) sorbitan monooleate (Tween® 80) was added to the resultant precipitate in the second sample. Tween® 80, which has been used to prevent Al_2O_3 and $BaTiO_3$ nanocrystal growth and agglomeration [21,22], has also carboxylic groups in its chemical structure [23]. The third sample was prepared without the addition of the surface modifying agent. A commercial micrometer Mn^{2+}-doped ZnS phosphor powder with a cubic phase was used as a reference.

Transmission electron microscopy (TEM) study of these nanocrystals was carried out at 200 kV using a Hitachi HF-2000 TEM equipped with a field emission source. The TEM specimens were prepared by dispersing the as-prepared Mn^{2+}-doped ZnS nanoparticles in methane, and picking up the nanocrystals using a carbon film supported by a copper grid. X-ray diffractometry (XRD) was performed using an XDS X-ray diffractometer (Model 2000, Scintag, Inc.) from $2\theta = 20^\circ$ to 80° with a scan step of 0.02°. The UV–visible absorption spectrum was obtained in a Hitachi 5000 spectrophotometer for Mn^{2+}-doped ZnS nanoparticles coated on a silica glass substrate. This sample was prepared by dip-coating from a colloidal solution of ZnS and drying at room temperature in air. Above band gap excitation PL measurements were performed using the 275 nm (4.51 eV) line of an argon ion laser. The laser power was reduced to an appropriate level by using a set of neutral density filters to avoid local heating. Typical excitation intensities were between $300\,mWcm^{-2}$ and $1\,Wcm^{-2}$. The PL signal was dispersed by a 1000 M Spex monochromator and detected by a thermoelectrically cooled GaAs photomultiplier tube (PMT) operating in the photon counting mode.

3. Results and discussion

HRTEM images in Figs. 1 and 2 show well-defined nanocrystals whose size was estimated to

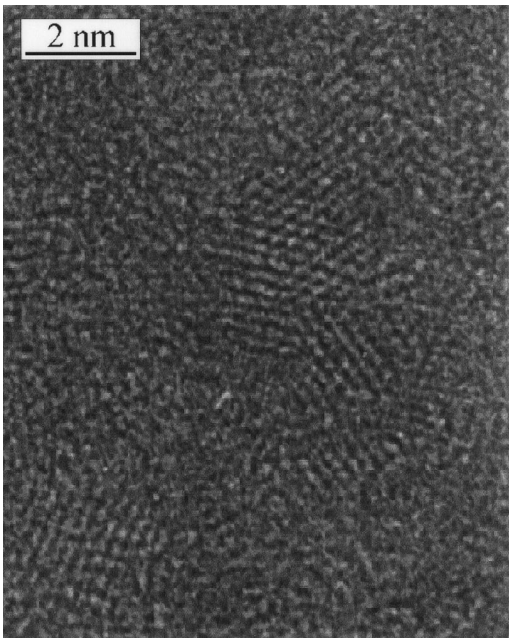

Fig. 1. HRTEM image of Mn^{2+}-doped ZnS nanoparticles.

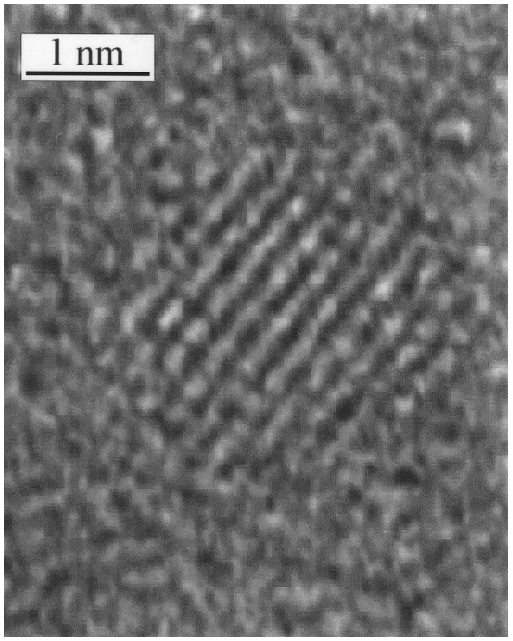

Fig. 2. HRTEM image of an individual Mn^{2+}-doped ZnS nanoparticle.

be about 2.8 nm. The lattice fringe is clearly exhibited from an individual nanocrystal, whose lattice constant d was evaluated as 3.11 Å (Fig. 2). This is in good agreement with lattice constant of cubic ZnS with a d of 3.123 Å for {1 1 1} plane. It is shown in Fig. 3 that XRD pattern of the nanocrystals is well matched with the standard cubic ZnS JCPDS No. 5-566 (vertical lines in Fig. 3). The peak broadening in the XRD pattern clearly indicates that very small nanocrystals are present in the samples. From the width of the XRD peak broadening, the mean crystalline size can be calculated using Scherrer's equation: $D = 57.3\,k\lambda/\beta\cos\theta$, where k is a geometric factor taken to be 1, λ is the X-ray wavelength (for Cu K_α radiation, $\lambda = 1.541$ Å), θ is the diffraction angle, and β is the half-width of the diffraction peak at 2θ. The mean crystal size of Mn^{2+}-doped ZnS nanoparticles is calculated to be 2.6 nm with a calculation error of 15%, i.e., 2.6 ± 0.4 nm. This is consistent with the estimated size from nanocrystals in HRTEM images. No apparent difference was observed in the XRD peak shape and broadening of Mn^{2+}-doped ZnS nanoparticles before and after surface passivation.

Fig. 4 exhibits the UV–visible absorption spectrum of Mn^{2+}-doped ZnS nanoparticles deposited on a silica glass substrate. This absorption spectrum exhibits a shoulder at 303 nm (4.09 eV), resulting from the quantum confinement effect of Mn^{2+}-doped ZnS nanoparticles. It suggests a large blue shift of 0.43 eV of the absorption band from that of 339 nm (3.66 eV)

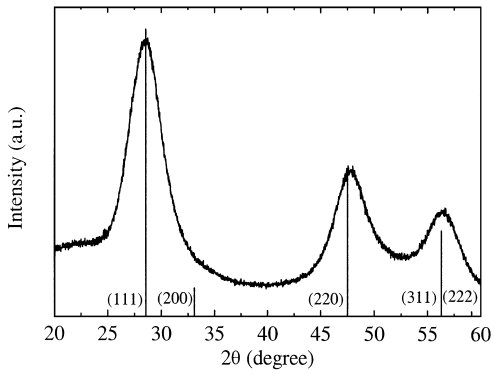

Fig. 3. XRD pattern of Mn^{2+}-doped ZnS nanoparticles (mean particle size 2.6 nm calculated from peak broadening).

for bulk ZnS crystals at room temperature [1,2]. Thus, the band gap of Mn^{2+}-doped ZnS nanoparticles has been enlarged. Since the crystallite size of Mn^{2+}-doped ZnS nanoparticles is smaller than double the Bohr radius of an exciton in bulk ZnS crystal, a quantum confinement effect is expected to occur within these nanocrystals, exhibiting an enlargement of the optical band gap [1,2].

PL properties of Mn^{2+}-doped ZnS nanoparticles were characterized for samples with MPTS, with Tween® 80, and without additives (Fig. 5). An orange photoluminescence was observed from Mn^{2+}-doped ZnS nanocrystals without MPTS whose peak is located at 601 nm. It is also shown in Fig. 5 that the PL intensity of Mn^{2+}-doped ZnS nanocrystals passivated by MPTS was enhanced by a 30-fold, in comparison with the samples without MPTS passivation. No orange photoluminescence from MPTS alone was observed after UV excitation at 275 nm. This confirms that the enhanced PL is not from MPTS itself but from surface passivated nanoparticles. In contrast, the PL intensity of Mn^{2+}-doped ZnS nanoparticles coated with Tween® 80 remained the same as that without the surface agent. This indicates that not all surface absorbates effective enhancing photoluminescence of Mn^{2+}-doped ZnS nanoparticles by surface passivation. Gallagher et al. [18] also did not observe any photoluminescence enhancement in Mn^{2+}-doped ZnS nanocrystals coated with poly ethylene oxide.

By comparison with the emission spectrum of micrometer size Mn^{2+}-doped ZnS phosphors, a red shift of the photoluminescence peak position is clearly seen (Fig. 6). The peak position shifts from 589 nm for micrometer size Mn^{2+}-doped ZnS phosphors to 601 nm for Mn^{2+}-doped ZnS nanoparticles without MPTS. This PL peak red shift to 601 nm from Mn^{2+}-doped ZnS nanoparticles was not reported by other researchers [1,2,6,20] despite Khosravi et al. [13] reported that

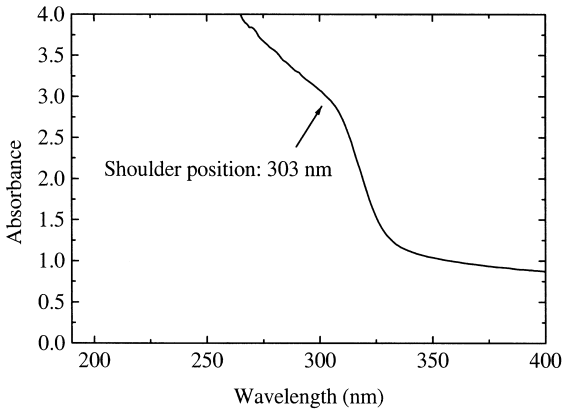

Fig. 4. Absorption spectrum of Mn^{2+}-doped ZnS nanoparticles on pure silica glass substrate.

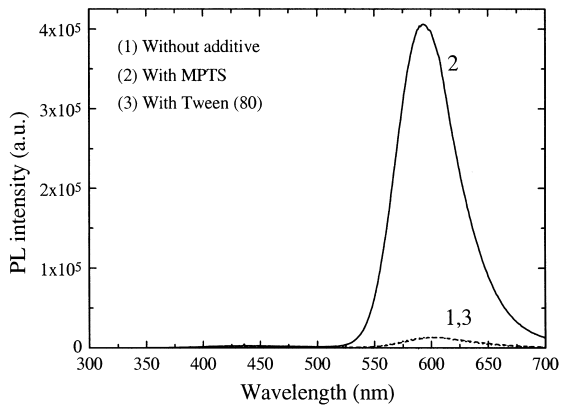

Fig. 5. Photoluminescence enhancement by a factor of 30 from Mn^{2+}-doped ZnS nanoparticles passivated by MPTS: (1) without MPTS, (2) with MPTS, and (3) with Tween® 80.

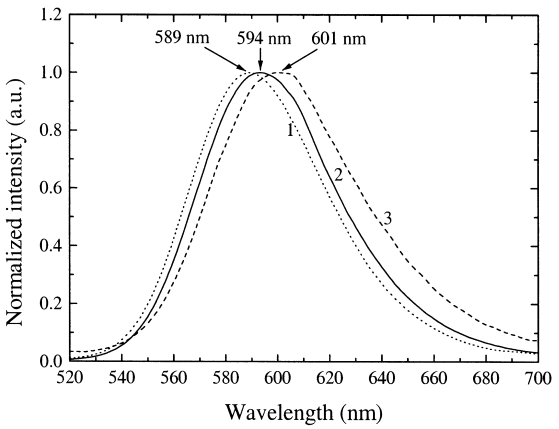

Fig. 6. Orange photoluminescence of (1) micrometer size Mn^{2+}-doped ZnS phosphors (peak position at 589 nm), (2) Mn^{2+}-doped ZnS nanoparticles with MPTS (peak position at 594 nm), and (3) Mn^{2+}-doped ZnS nanoparticles without MPTS (peak position at 601 nm).

the photoluminescence peak is located at ~ 600 nm from Mn^{2+}-doped ZnS nanoparticles with a mean size of 2.5 nm. Although it is still not certain that this red shift of the emission peak is due to the quantum confinement effect of the nanocrystals, it is believed that this red shift is related to small particle size, narrow size distribution, and/or surface defects. In contrast, the emission peak position shifts back to 594 nm for Mn^{2+}-doped ZnS nanocrystals after surface passivation using MPTS.

The orange photoluminescence originates from a transition between the $^4T_1$ excited state and the $^6A_1$ ground state of the Mn^{2+} ion within a nanocrystalline ZnS lattice. Due to the small particle size in 2.6 ± 0.4 nm, surface defects such as donors and acceptors are easily formed on the ZnS nanocrystal surface. When an electron is prompted to the excited state, there are two main paths for the electron to relax to the ground state. One is the relaxation process through surface defects, such as donors and acceptors. This relaxation will usually give rise to a non-radiative recombination and/or light emission at other wavelengths. The other emission is due to an intraconfigurational $3d^5$ transition on the Mn^{2+} ion located within the band gap of ZnS nanocrystals. This $^4T_1$–$^6A_1$ energy transition gives rise to an orange photoluminescence.

The PL enhancement can be explained by a passivation of the surface defects on nanoparticles. Since non-radiative recombination occurs through these surface defects, the radiative probability through the Mn^{2+} centers decreases with increasing surface defects. It is, therefore, expected that an enhancement of the radiative probability will be achieved by an elimination of the surface defects through surface passivation. In the presence of MPTS as a surface modifier, the surface defects on Mn^{2+}-doped ZnS nanoparticles are passivated and eliminated. Hence, an increase of the radiative transition through Mn^{2+} centers is accomplished. In other words, the 30-fold photoluminescence enhancement is caused by the eliminating of surface defects after surface passivation of the 2.6 ± 0.4 nm nanocrystals. Lunt et al. [24] observed increases of luminescence efficiency and decay lifetime in GaAs by passivating the surface recombination using organic thiols. Such chemical groups as Lewis bases (or electron donating groups), e.g., methoxides, increased the PL intensity of GaAs by reducing the non-radiative recombination on the surface. In $AlN:Er^{3+}$ PL could be increased by a factor of 5 when the surface was passivated by deuterium [25]. The intensity of visible PL from thin films of silicon nanoparticles was shown to be dependent upon the degree of surface passivation, while the emission energy was independent of the specific chemical nature of the passivation agent [26]. Seraphin et al. [26] explained this as the elimination of competing non-radiative carrier relaxation pathways. Such luminescence enhancement due to the surface passivation has also been reported for core–shell quantum-dots structures. Bruchez et al. [27] reported that by enclosing a core nanocrystals of one material with a shell of another having a larger band gap, one can efficiently confine the excitation to the core quantum dots, eliminating non-radiative relaxation pathways and enhancing photoluminescence.

MPTS plays an important role in eliminating the surface defects on Mn^{2+}-doped ZnS nanoparticles. In the literature [14,16,20], PL enhancement by MA or PMMA has been reported. Comparing MPTS with MA and PMMA, it is believed that the carboxylic groups from these surface-modifying agents play a significant role in enhancing the PL intensity. Isobe et al. [20] verified the chemical interaction between sulfur on $ZnS:Mn^{2+}$ nanoparticles surface and oxygen of carboxylic acid in MA by X-ray photoelectron spectroscopy (XPS). They concluded that the carboxylic group anchors on particle surface after formation of Mn^{2+}-doped ZnS nanoparticles. Surface passivation of the defects by the presence of a passivating coating is, therefore, achieved. However, not all surface passivating agents containing carboxylic functional groups showed PL enhancement effect for Mn^{2+}-doped ZnS nanoparticles. Tween® 80, a polyethylene of sorbitan oleate, played no role in PL enhancement. It is well known that the carboxylic-ester groups can have resonance structure and inductive effect by the chemical nature of the molecular structure. The resonance/inductive effect can be ineffective if there is a severe steric

hindrance. Tween® 80 does have the steric hindrance from long chains both sides of the carboxylic-ester group. It is believed that this steric hindrance hinders the adsorption of Tween® 80 molecules on the nanoparticle surface via the carboxylic-ester group. Hence, Tween® 80 must adsorb on nanoparticle surface via-OH groups. In comparing MPTS with Tween® 80, the resonance/inductive effect makes interaction of the carboxylic-ester group on nanoparticles enhanced, leading to a surface passivation of the nanoparticles in the presence of the functional group. On the other hand, poly ethylene oxide, which has no carboxylic groups in its long chain, has no luminescence enhancement effect for Mn^{2+}-doped ZnS nanoparticles [18].

4. Conclusion

Mn^{2+}-doped ZnS nanoparticles with enhanced photoluminescence have been synthesized by chemical precipitation at room temperature in the presence of MPTS as a surface-passivating agent. A 30-fold enhancement has been observed after the surface passivation. This is achieved by eliminating the surface defects, in which the carboxylic groups with effective resonance/inductive effect in the surface modifying agent plays an important role.

Acknowledgements

S.W. Lu and B.I. Lee wish to thank the financial support from American Chemical Society's Petroleum Research Fund type AC.

References

[1] R.N. Bhargava, D. Gallagher, T. Welker, J. Lumin. 60 and 61 (1994) 275.
[2] R.N. Bhargava, D. Gallagher, X. Hong, A. Nurmikko, Phys. Rev. Lett. 72 (1994) 416.
[3] Y. Yang, S. Xue, S. Li, J. Huang, J. Shen, Appl. Phys. Lett. 69 (3) (1996) 377.
[4] P.K. Sharma, R. Nass, H. Schmidt, Opt. Mater. 10 (1998) 161.
[5] E.T. Goldburt, B. Kulkarni, R.N. Bhargava, J. Taylor, M. Libera, J. Lumin. 72–74 (1997) 190.
[6] K. Sooklal, B.S. Cullum, S.M. Angel, C.J. Murphy, J. Phys. Chem. 100 (1996) 4551.
[7] J. Huang, Y. Yang, S. Xue, B. Yang, S. Liu, J. Shen, Appl. Phys. Lett. 70 (1997) 2335.
[8] R.N. Bhargava, US patent 5 455 489, October 3, 1995.
[9] U. Sohling, G. Jung, D. Saenger, S. Lu, B. Kutsch, M. Mennig, J. Sol–Gel Sci. Technol. 13 (1–3) (1998) 685.
[10] A.A. Bol, A. Meijerink, Phys. Rev. B 58 (1998) R15 997.
[11] N. Murase, R. Jagannathan, Y. Kanematsu, M. Watanabe, A. Kurita, K. Hirata, T. Yazawa, T. Kushida, J. Phys. Chem. B 103 (1999) 754.
[12] K. Sooklal, B. Cullum, S. Angel, C.J. Murphy, NATO ASI Series 3, Nanoparticles in solids and solutions, in: J. H. Fendler, I. Dekany (Eds.), Proceedings of the NATO Advanced Research Workshop, Vol. 18, 1996, pp. 455–465.
[13] A.A. Khosravi, M. Kundu, B.A. Kuruvilla, G.S. Shekhawat, R.P. Gupta, A.K. Sharma, P.D. Vyas, S.K. Kulkarni, Appl. Phys. Lett. 67 (1995) 2506.
[14] C. Jin, S. Hou, K. Dou, Y. Chen, S. Huang, J. Yu, Chinese Sci. Bull. 40 (1995) 1782.
[15] H. Yang, Z. Wang, L. Song, M. Zhao, Y. Chen, K. Dou, J. Yu, L. Wang, Mater. Chem. Phys. 47 (1997) 249.
[16] C. Jin, J. Yu, L. Sun, K. Dou, S. Hou, J. Zhao, Y. Chen, S. Huang, J. Lumin. 66 and 67 (1996) 315.
[17] L.M. Gan, B. Liu, C.H. Chew, S.J. Xu, S.J. Chua, G.L. Loy, G.Q. Xu, Langmuir 13 (1997) 6427.
[18] D. Gallagher, W.E. Heady, J.M. Racz, R.N. Bhargava, J. Crystal Growth 138 (1994) 970.
[19] Y. Wang, N. Herron, K. Moller, T. Bein, Solid State Commun. 77 (1991) 33.
[20] T. Isobe, T. Igarashi, M. Senna, Mater. Res. Soc. Symp. Proc. 452 (1997) 305.
[21] P.K. Sharma, M.H. Jilavi, D. Burgard, R. Nass, H. Schmidt, J. Am. Ceram. Soc. 81 (1998) 2732.
[22] S.W. Lu, B.I. Lee, Z.L. Wang, W.D. Samuels, J. Crystal Growth, in press.
[23] A.J.I. Ward, S.E. Friberg, J. Mater. Edu. 13 (1991) 113.
[24] S.R. Lunt, G.N. Ryba, P.G. Santangelo, N.S. Lewis, J. Appl. Phys. 70 (1991) 7449.
[25] S.J. Pearton, C.R. Abernathy, J.D. MacKenzie, U. Hömmerich, X. Wu, R.G. Wilson, R.N. Schwartz, J.M. Zavada, F. Ren, Appl. Phys. Lett. 71 (1997) 1807.
[26] A.A. Seraphin, S.T. Ngiam, K.D. Kolenbrander, J. Appl. Phys. 80 (1996) 6429.
[27] M. Bruchez Jr., M. Moronne, P. Gin, S. Weiss, A.P. Alivisatos, Science 281 (1998) 2013.